IEEE Access
Multidisciplinary | Rapid Review | Open Access Journal

Received 18 February 2024, accepted 14 March 2024, date of publication 18 March 2024, date of current version 25 March 2024.

Digital Object Identifier 10.1109/ACCESS.2024.3378739

RESEARCH ARTICLE

Hyperspectral Imaging Based Nonwoven Fabric Defect Detection Method Using LL-YOLOv5

HONGFEI LV, HONGRUI ZHANG, MENGKE WANG, JINHUAN XU, XIANGDONG LI, AND CHENGYE LIU

Institute of Automation, Qilu University of Technology (Shandong Academy of Sciences), Jinan, Shandong 250013, China

Corresponding author: Jinhuan Xu (jhxu@sdas.org)

This work was supported in part by the Pilot Special Basic Research Project for Science, Education, and Industry Integration, under Grant 2023PX061; in part by the Talent Scientific Research Project of Universities (Institutes) under Grant 2023RCKY156; in part by Shandong Provincial Natural Science Foundation under Grant ZR2022MF312; in part by the Major Innovation Fund of Qilu University of Technology (Shandong Provincial Academy of Sciences) under Grant 2022-JBZ02-02; and in part by Shandong Provincial Key Research and Development 23 Program under Grant 2021JMRHO108.

ABSTRACT Nonwoven fabric defect detection is an essential part of the production process, and it is important to realize fast and accurate nonwoven fabric defect detection to improve production efficiency. Aiming at the problems of nonwoven fabric defect detection in which most defect targets are small and traditional industrial cameras are unable to recognize foreign impurities of the same color, a nonwoven fabric defect detection method based on hyperspectral imaging and improved YOLOv5 is proposed. Specifically, hyperspectral imaging technology is used to replace traditional vision and solve the problem of homochromatic foreign matter impurities from the dimension of spectrum. In addition, the LSK attention module is introduced into the YOLOv5 backbone network, which enables the network to learn the key feature information and enhance the detection of small targets. Finally, an improved light repetitive group frequency permutation network (Light-RepGFPN) is proposed in the neck structure, by which the feature fusion capability of the model is enhanced, so that the high-level semantic information and the low-level spatial information are fully fused to improve the detection accuracy. Combined with the LSK and Light-RepGFPN modules, we propose an improved YOLOv5 (LL-YOLOv5) defect detection network. It is experimentally proved that LL-YOLOv5 can achieve an average accuracy mean 90.3% in the nonwoven fabric hyperspectral image defects dataset, which is 2.2% higher than that of the original model, respectively.

INDEX TERMS Attention mechanism, defect detection, hyperspectral imaging, YOLOv5.

I. INTRODUCTION

China as the country with the most complete types of cloth production, both production and export volume are ranked among the best in the world. The cloth production industry is one of the pillar industries of China's national economy [1]. As one of the fabrics, nonwoven fabrics are favored by users, whether in the industrial, agricultural, medical or daily decoration fields. As of 2020, the annual output of nonwoven fabrics in China has reached 6.76 million tons, and is showing a year-on-year increasing trend, and it is expected that the annual output of nonwoven fabrics will exceed 8 million tons by the end of 2024 [2]. Defects such as surface impurities, oil stains, wrinkles, holes and other defects will inevitably occur during the production process of cloth, thus weakening its expected performance and affecting its appearance. It is because of these defects that the quality and utility of cloth is greatly affected, so it is essential to carry out defect detection before the cloth leaves the factory.

The main application scenarios of nonwovens are: baby wipes, face wipes, disinfectant wipes, face masks, protective clothing and so on. It can be seen that most of the application scenarios of nonwoven fabrics are in direct contact with the skin, and most of the surface impurities are hard objects, which are very easy to scratch the skin, and the color of some surface impurities is very easy to confuse with the

The associate editor coordinating the review of this manuscript and approving it for publication was Kathiravan Srinivasan.

background color of nonwoven fabrics, which is difficult to be distinguished by the traditional visual inspection.

At present, for the defect detection of nonwoven fabrics, the classical machine vision method that combines edge detection and dynamic thresholding is mainly used [3], and the detection methods are fewer and more backward. Conventional methods for fabric defect detection are roughly divided into the following categories: structural texture-based methods [4], statistics-based methods [5], feature spectrum-based methods [6], feature model-based methods, and deep learning-based detection methods [7]. Seckin et al. [8] proposed a new feature extraction method by the intertwined frames for fabric defect detection, that is faster and provides higher accuracy. Cheng et al. [9] proposed a separation convolutional UNet combined with convolutional down sampling, depth separable convolution and cross-parallel ratio loss function (IoU loss), which performs the location detection of fabric defects by extracting the surface features in the fabric images, and performs well on the AITEX dataset. Compared to the other four traditional detection methods, deep learning-based detection methods can improve the detection effect and reduce the design cost.

Deep learning-based target detection algorithms can be categorized into one-stage target detection algorithms and two-stage target detection algorithms. Among the two-stage target detection algorithms, representative algorithms are fast region-based convolutional neural networks (Fast R-CNN) [10], faster region-based convolutional neural networks (Faster R-CNN) [11] and spatial pyramid pooling networks (SPP-Net) [12] algorithms. And the algorithmic process is as follows: Firstly, the convolutional neural network is used to carry out feature extraction. And then RPN (Region Proposal Network) network is used to generate the candidate region to realize the preliminary prediction of the target location. Finally, the ROI pooling layer is used to realize the precise location of the target, and the feature vector is generated through the fully connected layer to realize the determination of the target category and location through classification and regression. The two-stage detection algorithm has the advantages of high detection accuracy and high localization precision, but the detection speed is slow and not suitable for industrial real-time detection. Among the one-stage target detection algorithms, representative algorithms include: single shot multi box detector (SSD) [13], Retina Net [14], Efficient Det [15] and YOLO series [16], [17], [18], [19], [20], [21]. The one-stage target detection algorithm has two core parts, which are convolutional neural network and regression network, and the model can directly regress the category probability and location coordinates of the target. Thus, one-stage target detection algorithm has higher detection speed as the main research direction of defect detection at present. Liu et al. [22] strengthened the effect of detecting small target defects by adding a convolutional layer and a feature layer to the SSD algorithm. Zhang et al. [23] used YOLOv2 to achieve dyed fabric defect detection and classification based on deep convolutional neural network, which can extract defect features under the situation of limited samples. In order to solve the shortcomings of neural networks with large computational costs, which seriously impede the operation of the network in resource-limited environments, Liu et al. [24] proposed a lightweight convolutional neural network with a simple network structure, which has a substantial reduction in the amount of computation compared to the darknet feature extraction network. This method used two different scales for feature extraction, and the detection accuracy from the final results is slightly lower than the original. From the final results, the detection accuracy is slightly lower than the original YOLOv3 algorithm, but the detection speed is shortened to 38.5% of the original, which can be realized directly in the factory or embedded devices. In order to improve the defect detection rate and fabric product quality, Jing et al. [25] proposed a fabric defect detection method with higher real-time performance based on the improved YOLOv3 model, by adding a scale prediction layer, which makes the original three-scale prediction become four-scale prediction when the feature map is 104×104, the error rate of the improved network model for both gray and plaid fabrics are less than 5%. Zhu et al. [26] proposed to introduce the Transformer module as well as the convolutional attention module into the neck network and add a multi-scale feature detection layer, which makes the YOLOv5 network model to improve the detection accuracy of small targets and optimize the performance of the model, but the accuracy improvement is not obvious compared with the individual comparative models, and the introduction of the transformer module will increase the computational complexity and resource demand of the whole network. Zheng et al. [27] proposed the SE-YOLOv5 network, which adds squeeze and excitation network modules into the backbone of YOLOv5 and replaces the ReLU activation function in the CSP module, which improves the overall detection accuracy, but has a weak ability to detect insignificant defects. Liu et al. [28] introduced soft pooling into the YOLOv4 network model to improve the ability to detect fabric defects in tiny regions, but it also leads to an increase in the training and inference time of the model.

Li et al. [29] proposed a new hyperspectral imaging and modeling method, and an associated recognition model to classify single-component textiles, which extracts typical wavelength regions by band compression of data collected by hyperspectral imaging techniques, imports these data into a decision tree classifier and a KNN classifier for training, and develops a sample classification based on the training data recognition model. Chen et al. [30] realized the defect detection of Wet-Blue Leather with hyperspectral imaging technology, and enhanced the fusion of spectral and spatial information by segmenting the defective region with hyperspectral imaging technology and 1D convolutional neural network, 2D-Unet and 3D-UNet. These methods use

hyperspectral imaging for the first time for defect detection in fabrics, but the redundancy in the number of bands and the large number of processing parameters required require further research and improvement.

YOLOv5 is a high-performance single-stage target detection network, known for its speed and small model size and simple structure, so it is widely used in industrial production and life. However, blemishes vary in size and type, and some small blemish features are highly similar to the background information, which is difficult to be distinguished by the human eye. The direct application of YOLOv5 to nonwoven fabric defect detection is a significant challenge. Therefore, considering the tiny size and feature similarity of nonwoven defects, this paper proposes a nonwoven defect detection method based on hyperspectral imaging technology with improved YOLOv5.

The main contributions of this article are as follows:

1) The hyperspectral imaging technology is used to obtain the spectral information under different bands of nonwoven material and defects, analyze the difference of spectral information under different bands of nonwoven material and defects and select the key bands by feature extraction method to retain the separability information of nonwoven and defects, which effectively solves the problem of same-color foreign impurities.

2) The LSK Attention module is introduced into the Backbone network of YOLOv5, which can dynamically adjust its large spatial receptive field, enhance the defect feature extraction ability, strengthen the focus on the defective region, and increase the accuracy of small target detection.

3) The Light-RepGFPN network is proposed for constructing a new neck structure, which enables the network to exchange high-level semantic information and low-level spatial information more fully, and can increase the detection accuracy to a larger extent with a small amount of computational increase in the model.

The rest of the paper is organized as follows: Section II presents related work. Section III introduces the application of hyperspectral imaging for defect detection and describes the detection method in detail, including the overall network structure of LL-YOLOv5 and its individual modules. Section IV gives the experimental validation of our method. Section V summarizes our work and discusses the advantages and disadvantages of LL-YOLOv5 and related future research.

II. RELATED WORK

As one of the efficient single-stage detection networks, YOLOv5, has the advantage of more balanced detection accuracy and model complexity, and is widely used in various detection fields. In this paper, YOLOv5s-v7.0 released in December 2022 is used as the baseline model, and the network structure consists of four parts, namely, input, backbone, neck, and head, as shown in Figure 1.

The input part preprocesses the image, including Mosaic data enhancement, adaptive image scaling, and adaptive anchor frame design. The backbone network is a feature extraction sub-network, which is used to initially extract the features of the target image. The backbone network consists of CBS, C3, and SPPF modules. The C3 module is used for feature extraction. The SPPF module fuses the feature maps of different receptive fields. The neck network is the feature fusion sub-network, which fuses the extracted features. It consists of feature pyramid network (FPN) [31] and path aggregation network (PAN) [32]. The fusion process is that FPN up-samples deep features and fuses them with shallow features to enhance multi-scale semantic feature representation. PAN down-samples shallow detailed features and fuses them with deep features to enhance multi-scale localization. The head contains three detection layers corresponding to three different retarded feature maps. Predicting and regressing defective targets at different scales on the three medium feature maps.

III. HYPERSPECTRAL IMAGING BASED NONWOVEN FABRIC DEFECT DETECTION METHOD USING LL-YOLOv5

A. APPLICATION OF HYPERSPECTRAL IMAGING TECHNOLOGY IN NONWOVEN FABRIC DEFECT DETECTION

Hyperspectral imaging technology combines optics, spectroscopy and image processinag and other multidisciplinary knowledge, can obtain the spectral information of the object in different wavelength bands, providing rich spectral data. Traditional industrial camera is prone to miss the problem of wrong detection under the condition of the material of nonwoven fabrics and defects in the same or similar color in the defect detection process, and most of these defects are relatively hard metal or plastic, which is easy to scratch the skin in the use of the process, as shown in Figure 2. Hyperspectral imaging technology can effectively extract the spectral characteristics of the material of nonwoven fabrics and defects, which can be used to get the accurate detection and classification of nonwoven fabric defects by extracting and analyzing the spectral features. As shown in Figure 3, the red curve is the spectral data of the nonwoven fabric in the range of 900-1700nm, and the green curve is the spectral data of the foreign matter defects of the same color in the range of 900-1700nm, which are different and easy to distinguish.

Because the original hyperspectral data has a large amount of data, more bands, redundancy and other characteristics, which cannot be directly applied to the target detection algorithm. Therefore, according to the practical application of nonwoven fabric defect detection, this paper extracts three wavelengths (1202, 1421, 1540) and synthesizes the pseudo-RGB image by feature wavelength extraction, as shown in Figure 4, which effectively distinguishes the feature information of the nonwoven fabrics and defects and is convenient to be applied to the target detection algorithm.

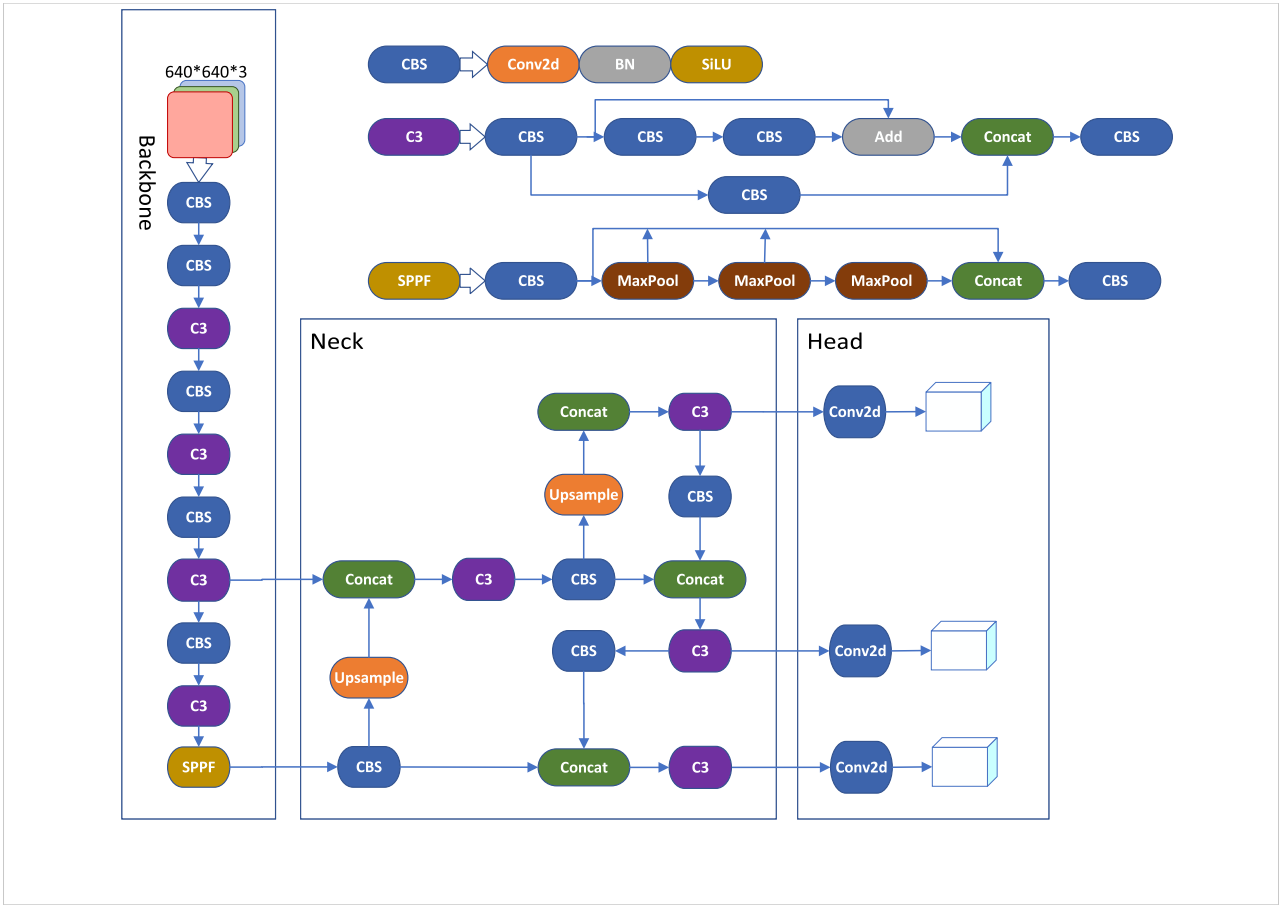

FIGURE 1. YOLOv5 network structure.

FIGURE 2. Blemishes similar to the background.

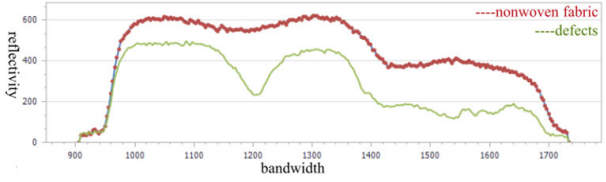

FIGURE 3. Spectral data curves of nonwovens and defects.

FIGURE 4. Pseudo-RGB image of same-color foreign matter defects after processing.

B. NONWOVEN FABRIC DEFECT DETECTION METHOD BASED ON LL-YOLOv5

In this paper, LSK Attention [33] is introduced into backbone in YOLOv5 to enhance the feature extraction capability of the backbone network. Referring to the Efficient RepGFPN structure in DAMO-YOLO [34], the Light-RepGFPN structure is proposed to replace the FPN+PAN structure of the original YOLOv5 network, and the addition of dimensionality reduction convolution (DC) reduces the number of network channels, so that the model obtains higher accuracy with a small number of parameters. Figure 5 shows the overall network model.

One of the difficulties in nonwoven fabric defect detection is that the defect targets are extremely small, which is easy to miss detection, and the shape of the defects is irregular and complex. LSK Attention module improves the accuracy of concern area by dynamically adjusting the spatial receptive field, which reduces the miss detection rate. Light-RepGFPN network makes the model more efficient when dealing with various sizes and complexities of targets by optimizing the feature representations. At the same time, considering that the hardware environment of the factory, the model volume and the number of parameters should be as small as possible, and the impact of either LSK Attention or Light-RepGFPN on the model volume and the number of parameters is minimal. Therefore, the integration of LSK Attention module and Light-RepGFPN network makes the LL-YOLOv5 model more powerful in the nonwoven fabric defect detection task.

1) LSK ATTENTION

The original backbone network may lead to the loss of important details and information when extracting features, in order to solve this problem, this paper refers to the LSK module and changes the large kernel convolutions to different kernel convolution sequences according to the different types of targets with different needs for background information. The convolutional sequences are embedded in the last layer of the backbone network, which fully explore the spatial structure information for fusion, and further improve the spatial features extraction of the model. The traditional spatial attention mechanism extracts spatial features with a single range of background information, which cannot guarantee the extraction of ideal spatial features. The main idea of LSK Attention is to effectively weight and spatially fuse the features under different receptive fields through different scale spatial information to obtain the final feature map. The structure of LSK Attention is shown in Figure 6. The main process of LSK Attention is:

In order to obtain rich background features from different regions of the input data X, convolution kernels with different receptive fields are used:

$$\mathbf{U}_0 = \mathbf{X}, \quad \mathbf{U}_1 = \mathcal{F}^{5\times5}(\mathbf{U}_0), \quad \mathbf{U}_2 = \mathcal{F}^{7\times7}(\mathbf{U}_1) \tag{1}$$

where $\mathcal{F}^{5\times5}$ is a Depth-wise convolution operation with a convolution kernel of 5, and $\mathcal{F}^{7\times7}$ is a Depth-wise convolution operation with a convolution kernel of 7 and an expansion rate of 3. The LSK attention dynamically selects an appropriate convolution kernel by considering the local information of the input feature map in order to adapt to the contextual information of various target types. It also adapts its receptive field dynamically to accommodate diverse target types and backgrounds. After that, each convolution operation is followed by another 1×1 convolution layer:

$$\tilde{\mathbf{U}}_i = \mathcal{F}_i^{1\times1}(\mathbf{U}_i) \tag{2}$$

Afterward, the feature maps are concatenated, depicted as follows:

$$\tilde{\mathbf{U}} = [\tilde{\mathbf{U}}_1; \tilde{\mathbf{U}}_2] \tag{3}$$

The spatial relationship are extracted by applying channel-level average pooling $\mathcal{P}_{avg}$ and maximum pooling $\mathcal{P}_{max}$:

$$\mathbf{SA}_{avg} = \mathcal{P}_{avg}(\tilde{\mathbf{U}}), \mathbf{SA}_{max} = \mathcal{P}_{max}(\tilde{\mathbf{U}}) \tag{4}$$

where $\mathbf{SA}_{avg}$ and $\mathbf{SA}_{max}$ are the spatial feature descriptors after average pooling and maximum pooling. After that, convolutional layers $\mathcal{F}^{2\to N}$ are utilized to transform them into spatial attention maps, and possess the same number of depth convolution N. The mathematical expression is:

$$\widehat{\mathbf{SA}} = \mathcal{F}^{2\to N}\left([\mathbf{SA}_{avg}; \mathbf{SA}_{max}]\right) \tag{5}$$

Afterwards, applying the sigmoid activation function to each spatial attention feature maps $\widehat{\mathbf{SA}}_i$, the spatial selection weights for each depth convolution are obtained.

$$\widetilde{\mathbf{SA}}_i = \sigma(\widehat{\mathbf{SA}}_i) \tag{6}$$

The weighted depth convolution feature maps are subsequently acquired by element-wise multiplication of the weights and the corresponding depth convolutions. Ultimately, a convolutional layer is employed to fuse these feature maps and produce the final attention feature. The mathematical expression is shown in Equations (7) and (8).

$$\mathbf{S} = \mathcal{F}(\sum_{i=1}^{\mathrm{N}}(\widetilde{\mathbf{SA}}_i \cdot \tilde{\mathbf{U}}_i)) \tag{7}$$

$$\mathbf{Y} = \mathbf{X} \cdot \mathbf{S} \tag{8}$$

In which, $\mathcal{F}$ is convolutional layer, $\mathbf{S}$ is the attention feature.

2) LIGHT-RepGFPN

It is crucial for a detector to learn sufficient fused information between high-level semantic and low level spatial features, which makes the detector neck to be a vital part of the whole framework. In [35], Generalized-FPN (GFPN) is proposed to serve as neck as it can sufficiently exchange high-level semantic information and low-level spatial information. In DAMO-YOLO, RepGFPN is designed with an accelerated queen-fusion, the efficient layer aggregation networks (ELAN) and re-parameterization. However, the RepGFPN structure will cause the number of parameters to drastically increase, thus affecting the detection efficiency. Based on RepGFPN, we propose a novel Light-RepGFPN to get the design of real-time object detection, instead of the original YOLOv5's FPN+PAN structure. Specifically, we adds the dimensionality reduction convolution before the structure, which effectively reduces the computation amount and the number of parameters, which improves the detection efficiency and makes the model have a smaller model volume to improve the detection accuracy. The overall structure is shown in Figure 7.

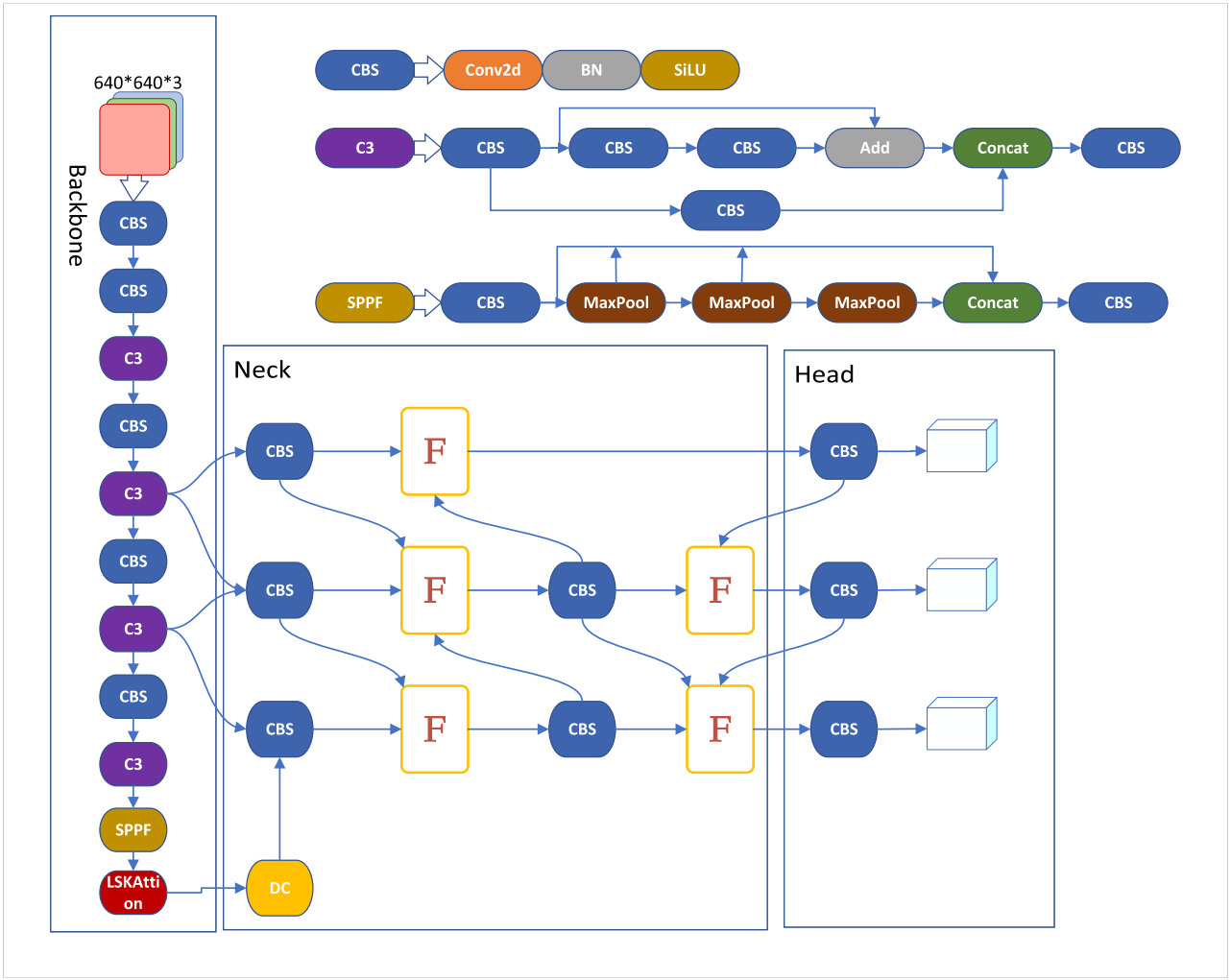

FIGURE 5. LL-YOLOv5 network structure.

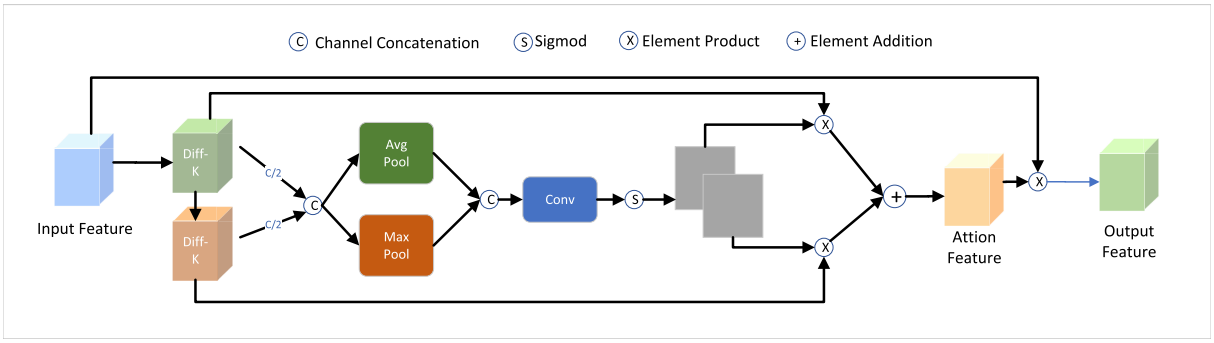

FIGURE 6. LSK attention.

In Figure 7, the meaning of CBS module is convolution, BatchNorm2d (normalization) and SILU activation function. F is the Fusion Block, and its structure is shown in Figure 8.

The inputs are two or three layers, which are concatenated and then channel dimensionality reduction is performed with convolution respectively, followed by a feature aggregation module that mimics ELAN, which consists of N Rep 3×3 convolutions and 3×3 convolutions, with simultaneous outputs from different layers, and then concatenated to get the final output.

Light-GFPN, based on Efficient-RepGFPN, fully combines both the contextual feature information to achieve

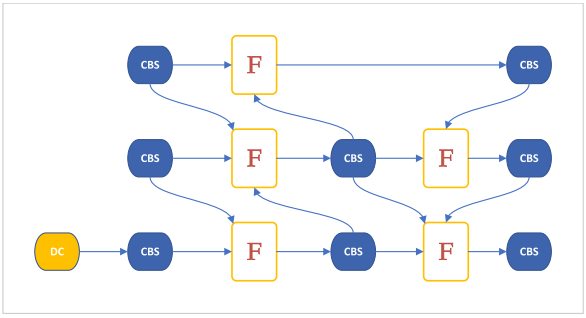

FIGURE 7. Light-RepGFPN.

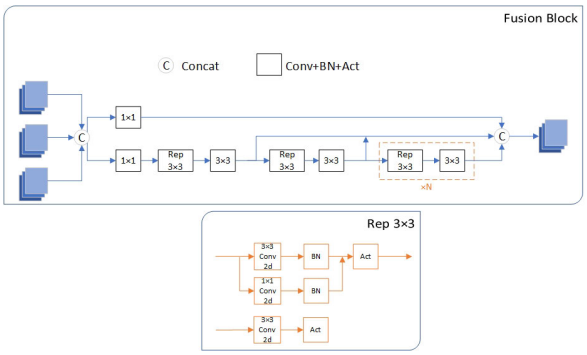

FIGURE 8. Fusion block.

higher detection accuracy and fully meets the lightweight requirements for real-time target detection.

IV. EXPERIMENT AND ANALYSIS

A. NONWOVEN FABRIC DEFECT DATASET

In order to facilitate data collection, this paper builds a nonwoven fabric data collection device for data collection, which is shown in Figure 9. The collection device includes a camera stand, a light source, a hyperspectral camera, collection station and acquisition system. The dataset used in this paper is the hydroentangled nonwoven fabric provided by Yongxin nonwoven factory and the defect samples generated in the actual production of the factory, and the nonwoven fabric is randomly combined with the defects in the collection station. And then the number of the data set was expanded to 4860 by the pre-processing methods such as scaling, rotating, adding noise, random color, etc. Figure 10 shows the preprocessed nonwoven image. The formats of the nonwoven fabric defects dataset images are all .PNG, and the number of training and test sets are 3985 and 875.

Defects are presented on the fabric that weaken its intended properties and affect its appearance. Crushing, friction, oil contamination and errors in the bleaching can affect the quality of the cloth, resulting in different types of defects. Common types of defects are surface impurities, oil stains, holes and folds.

(1) flaw: Generally metal impurities or fine particles due to machine friction, aging, rust during the production process.

(2) dirt: oil stains on the surface of nonwoven fabrics during the production process.

(3) fold: the crease produced by the extrusion.

(4) hole: the scratch on the surface of nonwoven fabrics after being scratched by sharp objects.

Figure 11 shows the nonwoven images containing defects of the used dataset. Figure 12 illustrates the number of each type of training defects.The dataset used in this paper contains 4860 images, of which the training set and test set is 3985+875, and the number of flaw for training and test is 5442+1229, the number of dirt for training and test is 276+51, the number of fold for training and test is 1158+285, the number of hole for training and test is 241+56.

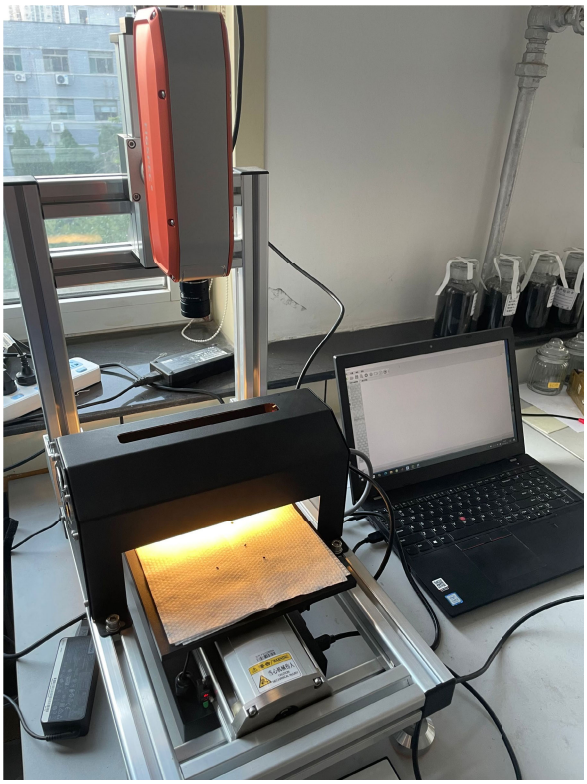

FIGURE 9. Nonwoven fabric data collection device.

FIGURE 10. Nonwoven fabric image. (a) original, (b) random invert, (c) invert+ add noise (d) invert+ random color.

B. PERFORMANCE METRICS

In order to verify the effectiveness of the algorithm proposed in this paper, Precision (P), Recall (R), Reconciliation Mean

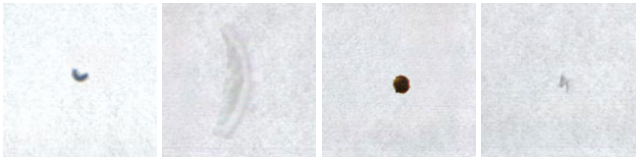

(a) (b) (c) (d)

FIGURE 11. Image of nonwoven fabric defects. (a)flaw, (b)fold, (c)dirt, (d)hole.

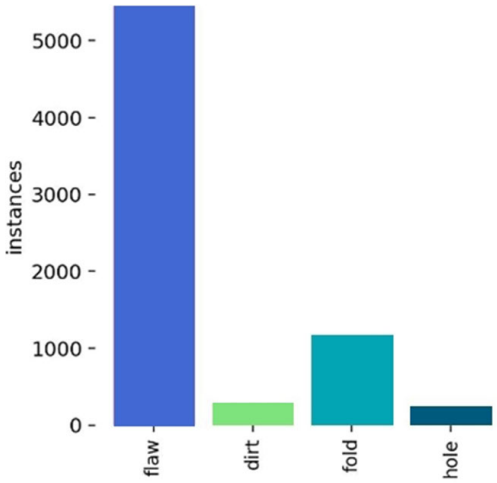

FIGURE 12. The number of various types of defects.

F1, Average Precision (AP), Mean Average Precision (mAP) are chosen as the evaluation indexes to measure the model performance. The amount of computation (GFLOPs) is used to measure the detection speed. The format of the dataset used in this paper is VOC. Therefore, mAP@0.5 is used as the primary measure, which indicates the mean AP at the IOU threshold of 0.5, which can directly reflect the detection ability of the model. The formulas for the above parameters are as follows.

$$P = \frac{TP}{TP + FP} \times 100\% \tag{9}$$

$$R = \frac{TP}{TP + FN} \times 100\% \tag{10}$$

$$F1 = \frac{2PR}{P + R} \times 100\% \tag{11}$$

$$AP = \int_0^1 P(R)dR \tag{12}$$

$$mAP = \frac{1}{K} \sum_{i=1}^{K} AP(i) \tag{13}$$

In which, TP is the number of correctly detected defects; FP is the number of misdetected defects; FN is the number of missed defects; TN is the detected background with a value of 0; K is the number of categories of defects.

C. SOFTWARE AND HARDWARE ENVIRONMENT SETTINGS

The experiments were conducted using Windows 10 operating system with a 12G NVIDIA GeForce RTX4070 GPU. The experimental platform is Anaconda + PyCharm, and the environment is configured with CUDA12.1, Python3.10, Pytorch2.1.0, torchvision0.16.0. The initial learning rate is 0.01, and its descent is by cosine annealing strategy, with a learning rate momentum of 0.937, a weight decay coefficient of 5e-4, and 32 Batchsize, trained with SGD optimizer for 100 iterations.

D. ABLATION EXPERIMENT

In order to verify the effect of the proposed LL-YOLOv5 model on f nonwoven fabric datasets, ablation experiments were conducted to evaluate the effectiveness of the improved modules under the same experimental environment and parameter settings. The ablation experiments consisted of four groups, which are shown in Table 1.

(1) YOLOv5 is the benchmark model before improvement, which serves as the comparison baseline for the following three groups of experiments.

(2) YOLOv5+LSK Attention is the experiment of adding LSK attention to the backbone network only. The LSK module effectively improves the feature extraction capability of the backbone network, resulting in 1.2% and 1.5% improvement in mAP@0.5 and mAP@0.5:0.95 values, respectively.

(3) YOLOv5+Light-RepGFPN is the experiment that only introduces Light-RepGFPN to replace the neck network, although the number of parameters and computation are increased, it can effectively improve the feature fusion ability of the network, which leads to an increase of 1.6% and 3.1% in the values of mAP@0.5 and mAP@0.5:0.95, respectively.

(4) LL-YOLOv5 is the experiment of the proposed method in this paper, adding both LSK Attention and Light-RepGFPN, which improves the accuracy P by 2.1%, the recall by 1.2%, and the mAP@0.5 and mAP@0.5:0.95 values by 2.2% and 4.0%, respectively, with limited increase in the number of parameters and the amount of computation of the model;

TABLE 1. Results of ablation experiments.

Group	P	R	mAP@0.5	mAP@0.5:0.95	GFLOPs
(1)	89.4%	84.2%	88.1%	59.2%	15.8G
(2)	89.7%	81.9%	89.3%	60.7%	16.1G
(3)	88.7%	88.4%	89.7%	62.3%	19.4G
(4)	91.5%	85.7%	90.3%	63.2%	20.1G

E. COMPARISON EXPERIMENTS

In this section, we conducted three types of comparative experiments. Firstly, the experiments are conducted to compare with four current mainstream attention mechanisms.

Secondly, the performance of the improved model is compared withthe benchmark model. Finally, the proposed method is compared with several mainstream classical detection methods.

1) COMPARATIVE EXPERIMENTS WITH DIFFERENT ATTENTION MECHANISMS

LSK Attention is compared with four mainstream attention mechanisms to verify the effectiveness of the attention mechanism in this paper, and the results are shown in Table 2. This experiment incorporates SE Attention Mechanism [36], CBAM Attention Mechanism [37], PSA Attention Mechanism [38], SSA Attention Mechanism [39] and LSK Attention Mechanism used in this paper, respectively, at the same location of the network and the same environment. It is experimentally verified that the attention mechanisms added in this paper are higher than other mainstream attention mechanisms in the mAP@0.5 index.

TABLE 2. Comparative experiments with different attention mechanisms.

Attention	P	R	mAP@0.5	mAP@0.95	GFLOPs
SE	89.6%	83.2%	88.3%	60.5%	15.8G
CBAM	90.0%	81.9%	88.9%	59.7%	16.2G
PSA	91.3%	84.0%	89.1%	61.0%	16.2G
SSA	87.3%	84.3%	87.9%	60.2%	16.2G
LSK	89.7%	81.9%	89.3%	60.7%	16.1G

2) PERFORMANCE COMPARISON EXPERIMENTS BETWEEN THE IMPROVED MODEL AND THE BENCHMARK MODEL

In order to prove that the proposed model in this paper has better detection effect than the benchmark model, the following comparison experiments are conducted. First, the graphs of mAP@0.5:0.95 values of the models are shown in Figure 13. After 100 training iterations, the detection accuracy of the proposed model has a smoother convergence curve during the training process, with smaller numerical fluctuations and higher accuracy, and the detection performance is better than the original model. In order to visualize whether the improved model is more accurate in identifying the critical locations of nonwoven defects, class activation maps are introduced to visualize the localization of defects. Figure 13 is the class activation maps for defect localization by the model before and after improvement, the darker red color means the more accurate localization of defects.

From Figure 14, it can be seen that the proposed method has higher corresponding to the defect site and is less disturbed by the background texture of the nonwoven fabric, indicating that is able to locate the defect area more accurately.

Table 3 shows the comparison of the detection performance on four different types of defects before and after the improvement, from which it can be seen that each type of defects has almost been improved on the mAP@0.5 index,

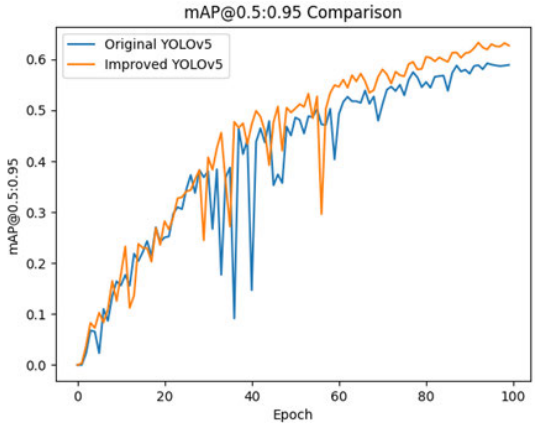

FIGURE 13. Comparison of mAP curves of models before and after improvement.

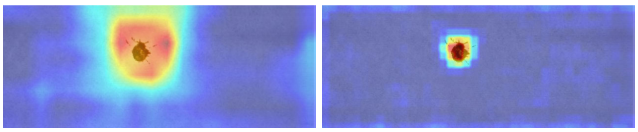

(a) (b)

FIGURE 14. Comparison of class activation maps for models before and after improvement. (a)YOLOV5, (b)LL-YOLOv5.

which indicates that the proposed model is also able to improve the detection accuracy on each type of defects compared with the original model.

TABLE 3. Comparison of mAP@0.5 indexes of defects detection results by category.

Defect type	mAP@0.5	
	YOLOv5	LL-YOLOv5
Flaw	98.2%	98.1%
Dirt	78.7%	82.4%
Fold	82.8%	86.8%
Hole	92.6%	94.0%

3) COMPARISON EXPERIMENTS WITH OTHER MAINSTREAM DETECTION METHODS

In this paper, the SSD, Faster-RCNN, YOLOv4, YOLOv5, YOLOv8 models are selected for comparison with LL-YOLOv5. (1) SSD, Faster-RCNN as classical models in the field of target detection are widely used in various application. (2) YOLOv4/5/8 represent different versions of the YOLO series in the development process, these models are chosen to track the evolution of the YOLO series and to evaluate the performance of LL-YOLOv5 in this series, and also to understand the competitiveness of LL-YOLOv5 against the emerging models, which is helpful to assess the latest research of LL-YOLOv5. (3) As described in the literature review of this paper, these models are widely used by researchers and scholars in the field of defect detection, and they are the mainstream models in the field of defect

detection at present, and comparing with these models, the advantages and disadvantages of the algorithm in this paper can be better reflected, as shown in Table 4.

From Table 4, compared with other detection models, the method proposed in this paper has a significant improvement in detection accuracy; and the volume of the improved model of this paper is relatively more advantageous. The model in this paper is better than SSD, Faster-RCNN, YOLOv4, YOLOv5 and YOLOv8 detection models in each parameter index, and can improve the detection accuracy under the condition of less parameter number. Taken together, the method in this paper is more advantageous in fabric defect detection.

Figure 15 illustrates the detection effect graph of LL-YOLOv5.

TABLE 4. Comparison of detection results of different methods.

Model	mAP@0.5	mAP@0.5:0.95	Model volume
Faster-RCNN	86.4%	56.2%	102.5MB
SSD	80.1%	49.6%	97.1MB
YOLOv4	86.1%	55.4%	18.7MB
YOLOv5	88.1%	59.2%	14.5MB
YOLOv8	90.1%	61.2%	22.5MB
LL-YOLOv5	90.3%	63.2%	20.0MB

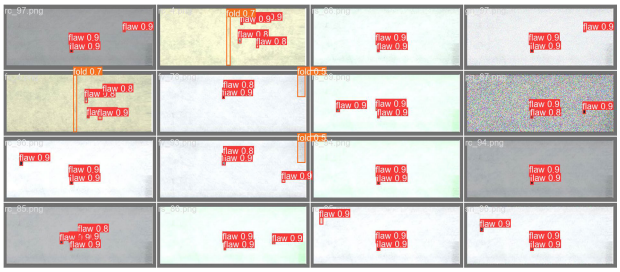

FIGURE 15. LL-YOLOv5 detection effect.

V. CONCLUSION

In order to further enhance the nonwoven fabric defect detection effect, this paper proposes a nonwoven fabric defect detection method based on hyperspectral imaging technology and improved yolov5, which strengthens the extraction ability of the backbone network on defect features by introducing LSK attention mechanism, and at the same time, the Light-RepGFPN feature fusion network is added into the neck structure, which effectively improves the degree of feature fusion. The experimental results show that the proposed LL-YOLOv5 detection method has more advantageous detection performance than other typical detection methods. Our preliminary thoughts on future research directions are as follows: Firstly, we will work on further improving the model performance on small target detection, which may involve new network structure, feature extraction methods and training strategies more suitable for small targets. Secondly, considering the diversity of different industrial environments and application scenarios, we will explore its applicability in real industries. This may include the introduction of domain-adaptive learning techniques to mitigate performance degradation due to environmental changes.

REFERENCES

[1] S. J. Russell, *Handbook of Nonwovens*. Sawston, U.K.: Woodhead Publishing, 2022.

[2] K. B. Yilmaz, B. Sabuncuoglu, B. Yildirim, and V. V. Silberschmidt, "A brief review on the mechanical behavior of nonwoven fabrics," *J. Engineered Fibers Fabrics*, vol. 15, Jan. 2020, Art. no. 155892502097019.

[3] K. L. Mak, P. Peng, and K. F. C. Yiu, "Fabric defect detection using morphological filters," *Image Vis. Comput.*, vol. 27, no. 10, pp. 1585–1592, Sep. 2009.

[4] A. Abouelela, H. M. Abbas, H. Eldeeb, A. A. Wahdan, and S. M. Nassar, "Automated vision system for localizing structural defects in textile fabrics," *Pattern Recognit. Lett.*, vol. 26, no. 10, pp. 1435–1443, Jul. 2005.

[5] G. Gao, D. Zhang, C. Li, Z. Liu, and Q. Liu, "A novel patterned fabric defect detection algorithm based on GHOG and low-rank recovery," in *Proc. IEEE 13th Int. Conf. Signal Process. (ICSP)*, Nov. 2016, pp. 1118–1123.

[6] S. Guan and X. Shi, "Fabric defect detection based on wavelet decomposition with one resolution level," in *Proc. Int. Symp. Inf. Sci. Eng.*, Dec. 2008, pp. 281–285.

[7] A. Basu, J. K. Chandra, P. K. Banerjee, S. Bhattacharyya, and A. K. Datta, "Sub image based eigen fabrics method using multi-class SVM classifier for the detection and classification of defects in woven fabric," in *Proc. 3rd Int. Conf. Comput., Commun. Netw. Technol. (ICCCNT)*, Jul. 2012, pp. 1–6.

[8] A. Ç. Seçkin and M. Seçkin, "Detection of fabric defects with intertwined frame vector feature extraction," *Alexandria Eng. J.*, vol. 61, no. 4, pp. 2887–2898, Apr. 2022. [Online]. Available: https://www.sciencedirect.com/science/article/pii/S1110016821005329

[9] L. Cheng, J. Yi, A. Chen, and Y. Zhang, "Fabric defect detection based on separate convolutional UNet," *Multimedia Tools Appl.*, vol. 82, no. 2, pp. 3101–3122, Jan. 2023.

[10] R. Girshick, "Fast R-CNN," in *Proc. IEEE Int. Conf. Comput. Vis. (ICCV)*, Dec. 2015, pp. 1440–1448.

[11] S. Ren, K. He, R. Girshick, and J. Sun, "Faster R-CNN: Towards real-time object detection with region proposal networks," in *Proc. Adv. Neural Inf. Process. Syst.*, vol. 28, 2015, pp. 1–7.

[12] K. He, X. Zhang, S. Ren, and J. Sun, "Spatial pyramid pooling in deep convolutional networks for visual recognition," *IEEE Trans. Pattern Anal. Mach. Intell.*, vol. 37, no. 9, pp. 1904–1916, Sep. 2015.

[13] W. Liu, D. Anguelov, D. Erhan, C. Szegedy, S. Reed, C. Fu, and A. Berg, "SSD: Single shot multibox detector," in *Proc. Eur. Conf. Comput. Vis.* Cham, Switzerland: Springer, 2016, pp. 21–37.

[14] T.-Y. Lin, P. Goyal, R. Girshick, K. He, and P. Dollár, "Focal loss for dense object detection," in *Proc. IEEE Int. Conf. Comput. Vis. (ICCV)*, Oct. 2017, pp. 2999–3007.

[15] M. Tan, R. Pang, and Q. V. Le, "EfficientDet: Scalable and efficient object detection," in *Proc. IEEE/CVF Conf. Comput. Vis. Pattern Recognit. (CVPR)*, Jun. 2020, pp. 10778–10787.

[16] J. Redmon, S. Divvala, R. Girshick, and A. Farhadi, "You only look once: Unified, real-time object detection," in *Proc. IEEE Conf. Comput. Vis. Pattern Recognit. (CVPR)*, Jun. 2016, pp. 779–788.

[17] J. Redmon and A. Farhadi, "YOLO9000: Better, faster, stronger," in *Proc. IEEE Conf. Comput. Vis. Pattern Recognit. (CVPR)*, Jul. 2017, pp. 6517–6525.

[18] J. Redmon and A. Farhadi, "YOLOv3: An incremental improvement," 2018, *arXiv:1804.02767*.

[19] A. Bochkovskiy, C.-Y. Wang, and H.-Y. M. Liao, "YOLOv4: Optimal speed and accuracy of object detection," 2020, *arXiv:2004.10934*.

[20] Z. Ge, S. Liu, F. Wang, Z. Li, and J. Sun, "YOLOX: Exceeding YOLO series in 2021," 2021, *arXiv:2107.08430*.

[21] C.-Y. Wang, A. Bochkovskiy, and H.-Y.-M. Liao, "YOLOv7: Trainable bag-of-freebies sets new state-of-the-art for real-time object detectors," in *Proc. IEEE/CVF Conf. Comput. Vis. Pattern Recognit. (CVPR)*, Jun. 2023, pp. 7464–7475.

[22] Z. Liu, S. Liu, C. Li, S. Ding, and Y. Dong, "Fabric defects detection based on SSD," in *Proc. 2nd Int. Conf. Graph. Signal Process.*, Oct. 2018, pp. 74–78.

[23] H.-W. Zhang, L.-J. Zhang, P.-F. Li, and D. Gu, "Yarn-dyed fabric defect detection with YOLOV2 based on deep convolution neural networks," in *Proc. IEEE 7th Data Driven Control Learn. Syst. Conf. (DDCLS)*, May 2018, pp. 170–174.
[24] Z. Liu, J. Cui, C. Li, M. Wei, and Y. Yang, "Fabric defect detection based on lightweight neural network," in *Proc. Chin. Conf. Pattern Recognit. Comput. Vis. (PRCV)*. Cham, Switzerland: Springer, 2019, pp. 528–539.
[25] J. Jing, D. Zhuo, H. Zhang, Y. Liang, and M. Zheng, "Fabric defect detection using the improved YOLOv3 model," *J. Engineered Fibers Fabrics*, vol. 15, Jan. 2020, Art. no. 155892502090826.
[26] X. Zhu, S. Lyu, X. Wang, and Q. Zhao, "TPH-YOLOv5: Improved YOLOv5 based on transformer prediction head for object detection on drone-captured scenarios," in *Proc. IEEE/CVF Int. Conf. Comput. Vis. Workshops (ICCVW)*, Oct. 2021, pp. 2778–2788.
[27] L. Zheng, X. Wang, Q. Wang, S. Wang, and X. Liu, "A fabric defect detection method based on improved YOLOv5," in *Proc. 7th Int. Conf. Comput. Commun. (ICCC)*, Dec. 2021, pp. 620–624.
[28] Q. Liu, C. Wang, Y. Li, M. Gao, and J. Li, "A fabric defect detection method based on deep learning," *IEEE Access*, vol. 10, pp. 4284–4296, 2022.
[29] J. Li, X. Meng, W. Wang, and B. Xin, "A novel hyperspectral imaging and modeling method for the component identification of woven fabrics," *Textile Res. J.*, vol. 89, no. 18, pp. 3752–3767, Sep. 2019.
[30] S.-Y. Chen, Y.-C. Cheng, W.-L. Yang, and M.-Y. Wang, "Surface defect detection of wet-blue leather using hyperspectral imaging," *IEEE Access*, vol. 9, pp. 127685–127702, 2021.
[31] G. Ghiasi, T.-Y. Lin, and Q. V. Le, "NAS-FPN: Learning scalable feature pyramid architecture for object detection," in *Proc. IEEE/CVF Conf. Comput. Vis. Pattern Recognit. (CVPR)*, Jun. 2019, pp. 7029–7038.
[32] L. Zhou, X. Rao, Y. Li, X. Zuo, B. Qiao, and Y. Lin, "A lightweight object detection method in aerial images based on dense feature fusion path aggregation network," *ISPRS Int. J. Geo-Inf.*, vol. 11, no. 3, p. 189, Mar. 2022.
[33] Y. Li, Q. Hou, Z. Zheng, M.-M. Cheng, J. Yang, and X. Li, "Large selective kernel network for remote sensing object detection," 2023, *arXiv:2303.09030*.
[34] X. Xu, Y. Jiang, W. Chen, Y. Huang, Y. Zhang, and X. Sun, "DAMO-YOLO: A report on real-time object detection design," 2022, *arXiv:2211.15444*.
[35] Y. Jiang, Z. Tan, J. Wang, X. Sun, M. Lin, and H. Li, "GiraffeDet: A heavy-neck paradigm for object detection," 2022, *arXiv:2202.04256*.
[36] J. Hu, L. Shen, and G. Sun, "Squeeze-and-excitation networks," in *Proc. IEEE/CVF Conf. Comput. Vis. Pattern Recognit.*, Jun. 2018, pp. 7132–7141.
[37] S. Woo, J. Park, J.-Y. Lee, and I. S. Kweon, "CBAM: Convolutional block attention module," in *Proc. Eur. Conf. Comput. Vis.*, Sep. 2018, pp. 3–19.
[38] H. Liu, F. Liu, X. Fan, and D. Huang, "Polarized self-attention: Towards high-quality pixel-wise regression," 2021, *arXiv:2107.00782*.
[39] S. Ren, D. Zhou, S. He, J. Feng, and X. Wang, "Shunted self-attention via multi-scale token aggregation," in *Proc. IEEE/CVF Conf. Comput. Vis. Pattern Recognit. (CVPR)*, Jun. 2022, pp. 10843–10852.

HONGFEI LV received the B.S. degree in electrical engineering and automation from Shandong Institute of Petroleum and Chemical Technology, Shandong, China, in 2022. He is currently pursuing the master's degree with the Institute of Automation, Qilu University of Technology (Shandong Academy of Sciences). His current research interest includes deep learning.

HONGRUI ZHANG received the B.S. degree in electrical engineering and automation from Linyi University, Shandong, China, in 2022. She is currently pursuing the master's degree with the Institute of Automation, Qilu University of Technology (Shandong Academy of Sciences). Her current research interest includes hyperspectral image processing.

MENGKE WANG received the B.S. degree in electrical engineering and automation from Shandong Jiaotong University, Shandong, China, in 2022. He is currently pursuing the master's degree with the Institute of Automation, Qilu University of Technology (Shandong Academy of Sciences). His current research interest includes hyperspectral image processing.

JINHUAN XU received the B.S. and Ph.D. degrees in computer science and technology from Nanjing University of Science and Technology, Nanjing, China, in 2014 and 2022, respectively. She has been an Research Assistant with the Institute of Automation, Qilu University of Technology (Shandong Academy of Sciences), Jinan, since 2022. Her research interests include remote sensing image processing and remote sensing information extraction and application.

XIANGDONG LI is the Director of the Intelligent Sensing Research Laboratory, Institute of Automation, Qilu University of Technology (Shandong Academy of Sciences), specializing in control engineering and robotics. He has participated in the development of the first national substation equipment inspection robot. He has presided over and participated in a number of provincial and ministerial level projects of research projects. He undertook a number of horizontal research projects. He was appointed as the deputy director of science and technology in Lanshan, Linyi, with excellent appraisal. He was honored as an advanced individual in Shandong Province's science and technology deputy work. He has published one monograph, the series won the 32nd East China Science and Technology Press Excellent Science and Technology Books First Prize. He has been authorized more than 20 patents and published more than 20 papers.

CHENGYE LIU is the Deputy Director, an Associate Researcher, and a Master's Tutor with the Institute of Automation, Qilu University of Technology (Shandong Academy of Sciences). For many years, he has been engaged in the research of mobile robot technology and sensing system technology. He has undertaken or participated in more than ten scientific research projects, including National Science and Technology Cooperation Projects and the Key Research and Development Projects in Shandong Province; three patents have been authorized; more than ten papers have been published; and two monographs have been published.